Time-frequency based nonstationary interference suppression for noise radar systems

Miloš Daković, Thayaparan Thayananthan, Slobodan Djukanović, Ljubiša Stanković

Abstract— **The problem addressed in this paper is nonstationary interference suppression in noise radar systems. Towards this aim, two linear time-frequency (TF) transforms, short time Fourier transform (STFT) and local polynomial Fourier transform (LPFT) are used as a means of signal representation and filtering. The noise radar return signal is a wideband random signal occupying the whole TF plane, while the interference signal is well concentrated in the TF plane. This implies that the filtering of the received signal can be performed by using a binary mask to excise only a portion of the TF plane corrupted by the interference. Simulations carried out on the radar return signal corrupted by extremely strong nonstationary interferences confirm the effectiveness of the proposed method.**

I. Introduction

The term "random noise" as applied to radar refers to techniques and applications that use incoherent noise as the probing transmitted waveform. Because of the truly random transmitting signal, noise radars have many advantages over conventional radars, including unambiguous estimation of both range and velocity, high immunity to noise, low probability of intercept (LPI), high electromagnetic compatibility, good electronic counter countermeasure (ECCM) capability, good counter electronic support measure (CESM) capability, and ideal thumbtack ambiguity function [1]-[12].

Over the past few years, the research has been devoted to the development and implementation of random noise radar by various research groups [4], [7], [8], [9]. Recent research has investigated the potential use of noise radar for ultrawideband SAR/ISAR imaging, Doppler and polarimetric measurements, collision warning, detection of buried objects, and targets obscured by foliage [2], [5], [8]-[11]. Wide bandwidth provides a high range resolution, and an extended pulse length reduces peak power. The non-periodic waveform suppresses the range ambiguity while reducing both the probability of intercept and interference.

Mutual interference and low probability of interception capabilities of noise radar were evaluated in previous studies. The results show that noise radars are unlikely to interfere with other noise radar systems or other radar systems in the same band. It is also shown that in a variety of noisy environments, the noise radar has a much lower LPI than the conventional LFM radar. The noise radar's exceptional performance in the above evaluations indicates that it is a suitable radar system for a variety of applications frequently improving upon the performance of conventional systems [12], [13].

In this paper we have studied the influence of an extremely strong deterministic broadband interference (signal-to-interference ratio as low as -40dB), covering the frequency and time ranges of the operating noise radar. A time-frequency (TF) based interference suppression technique is developed and is based on the property of TF representations to localize signals in the TF plane. Two TF transforms, the short time Fourier transform (STFT) and the local polynomial Fourier transform (LPFT), are herein used. More precisely, time-varying filters based on the STFT and LPFT are developed. Since the random noise radar

IET Radar, Sonar and Navigation, Vol. 2, No. 4, Aug. 2008.

signal occupies the whole TF plane, whereas the interference signal is a broadband signal characterized with a narrow instantaneous bandwidth, the time-varying filtering is performed via binary masking, as a means of removing the TF signature of the interference without significant degradation of the radar return signal. Moreover, the LPFT based receiver outperforms the STFT based receiver since it optimally concentrates an interference in the TF plane. Numerical simulations consider two types of interferences, that is, broadband sinusoidal frequency modulated (SFM) and linear frequency modulated (LFM) interferences. The latter may be viewed as an interfering LFM radar, covering the same time and frequency ranges as the operating noise radar.

The theoretical background, including the STFT, the LPFT, time varying filtering, and correlation-based noise radar principles, is given in Section 2. Section 3 introduces two methods for binary mask implementation. The proposed TF filtering methods' performances are evaluated by means of numerical examples in Section 4. It has been shown that the noise radar implementing the proposed filtering method performs satisfactorily, even in a severe interfering environment.

II. Theoretical background

In this section, a short introduction to linear TF methods, i.e., the STFT and LPFT, is given. Furthermore, the section also provides a brief description of time-varying filtering and correlation based noise radar principles.

The baseband received signal $r(n)$ comprises three sequences as follows:

$$r(n) = x(n) + I(n) + \xi(n) \tag{1}$$

where $x(n)$ is a noise radar signal sequence (complex white Gaussian noise sequence with zero mean and variance σ_x^2), $I(n)$ is an interference signal sequence and $\xi(n)$ is a complex additive white Gaussian noise (AWGN) sequence, with zero mean and variance σ_ξ^2. All the sequences are uncorrelated with each other. The interference is assumed to be a nonstationary signal characterized by a narrowband instantaneous bandwidth and the following analytical expression:

$$I(n) = A_I e^{j\varphi_I(n)}$$

where $\varphi_I(n)$ is the phase and A_I is the magnitude of the interference.

Signal-to-noise ratio (SNR) and signal-to-interference ratio (SIR) are defined in the following way:

$$SNR = 20\log_{10}\frac{\sigma_x}{\sigma_\xi} \tag{2}$$

$$SIR = 20\log_{10}\frac{\sigma_x}{A_I}. \tag{3}$$

The influence of the interference signal on the desired radar signal can be mitigated by using TF methods. Herein, we are interested only in linear TF methods, that allow the perfect reconstruction (synthesis) of the observed signal. Two such methods, i.e., short-time Fourier transform and local polynomial Fourier transform, will be used as a means of interference suppression in this paper.

A. Short-time Fourier transform

The STFT of the signal $r(n)$ [15], denoted as $STFT_r(n,k)$, is obtained by sliding the window function $w(m)$ over the signal $r(n)$ and implementing the DFT on the product of $r(n)$ and window at the current position, i.e.,

$$\begin{aligned} STFT_r(n,k) &= \\ \sum_{m=-N/2}^{N/2-1} & r(n+m)\,w(m)\,e^{-j\frac{2\pi}{N}mk} \\ &= DFT\left[r(n+m)\,w(m)\right] \end{aligned} \tag{4}$$

where N is the number of frequency bins adopted in the DFT calculation. The window function is usually real and symmetric with the property $w(0) = 1$. A simple manipulation of (4) gives the STFT synthesis equation

$$r(n) = \frac{1}{N}\sum_{k=0}^{N-1} STFT_r(n,k). \tag{5}$$

This relation states that the signal $r(n)$ can be obtained by summing STFT values over the frequency variable k for the fixed time instant n.

B. Local polynomial Fourier transform

The LPFT has been recently introduced in the TF analysis [16], [17], with the Mth order discrete form of the LPFT of the sequence $r(n)$ being defined as

$$LPFT_r^M(n,k) = \sum_{m=-N/2}^{N/2-1} r(n+m)w(m)\, e^{-j\sum_{i=1}^{M}\omega_i \frac{m^{i+1}}{(i+1)!}} e^{-j\frac{2\pi}{N}mk} = DFT\left(r(n+m)w(m)\, e^{-j\sum_{i=1}^{M}\omega_i \frac{m^{i+1}}{(i+1)!}}\right) \quad (6)$$

where $w(m)$ and N are the same as in the STFT definition and ω_i is the ith transform parameter. The relation (6) indicates that the LPFT of the received signal can be calculated analogously to the STFT, i.e., by sliding the analysis window $w(m)$ over the modulated received signal

$$r(n+m)e^{-j\sum_{i=1}^{M}\omega_i \frac{m^{i+1}}{(i+1)!}}$$

and implementing the DFT on the product of the modulated signal and window at the current position.

The LPFT parameters ω_i for $i = 1, 2, ..., M$ are calculated so as to optimally concentrate the signal (i.e., interference in this case) in the TF plane for a given analysis window. Towards this goal, an order adaptive algorithm is developed in [16] and it is shown to keep calculation complexity at a relatively low level. Furthermore, it is shown that the second-order LPFT produces results almost independent of the parameters of an FM interference, thus preventing the need for a time-consuming calculation of the higher-order LPFT.

C. Time-varying filtering: Binary mask

The spectrum of the noise radar signal is flat, while the interference signal occupies a narrow frequency band at each time instant. The time-varying filtering described in [14] can be easily herein implemented. The interference excision is performed in the TF plane by removing its TF signature through a time-varying filter. This filter can be implemented as a binary mask, denoted as **B**, which is a function defined in the following way:

$$B(n,k) = \begin{cases} 0, & \text{interference exists in } (n,k) \\ 1, & \text{otherwise.} \end{cases} \quad (7)$$

Practically, $B(n,k)$ will equal 1 only for points (n,k) of the TF plane where the interference power can be neglected.

The synthesis is performed on the masked transform to recover the "jammer-free" received signal $r'(n)$ as follows:

$$r'(n) = \frac{1}{N}\sum_{k=0}^{N-1} STFT_r(n,k)B(n,k) \quad (8)$$

or

$$r'(n) = \frac{1}{N}\sum_{k=0}^{N-1} LPFT_r^M(n,k)B(n,k). \quad (9)$$

D. Correlation Receiver

The correlation receiver uses the principle that when the reference signal, delayed by T_{ref}, is correlated with the actual target echo, the peak value of the correlation function indicates the distance to the target (the amount of time delay of the reference signal is also a measure of distance to the target), while Doppler filters, following the correlator, output the target velocity [7]. In this method, the return signal from the target is cross-correlated with a time-delayed replica of the transmit waveform. When T_{ref} is varied a strong correlation peak is obtained for $T_{ref} = T_0$, which gives an estimate of the target range $r_0 = cT_0/2$.

Let us consider a radar emitting a time-limited signal $x(t)$. Denote the received signal by $y(t)$. Furthermore, we assume that a single point scatterer is located at the range r_0 along the radar line-of-sight (LOS). From this assumption, the received signal can be written as:

$$y(t) = A_\sigma x(t - T_0) + \varepsilon(t) \quad (10)$$

where $T_0 = 2r_0/c$ is the round-trip delay caused by the finite speed of the electromagnetic waves, $\varepsilon(t)$ is an undesired part of the received signal (noise caused by the reflection from other objects along the LOS and possible jamming signals) with A_σ denoting target

reflectivity. Without loss of generality we will assume that $A_\sigma = 1$. The correlation of the emitted and received signal can be written as:

$$R(\tau) = \int_0^{T_{int}} y(t)x^*(t-\tau)dt. \qquad (11)$$

where T_{int} is the integration time. In the noiseless case, the maximum value of $|R(\tau)|$ occurs at the point $\tau = T_0$.

Let us now assume that $x(t)$ is a stationary Gaussian random process with autocorrelation function $R_{xx}(\tau)$. Due to the finite integration time T_{int}, the output of the correlation receiver given by (11) is also a random process. Let us analyze the expected value of (11) as:

$$\begin{aligned} E[R(\tau)] &= E[\int_0^{T_{int}} y(t)x^*(t-\tau)dt] \\ &= \int_0^{T_{int}} E[y(t)x^*(t-\tau)]dt \\ &= \int_0^{T_{int}} (E[x(t-T_0)x^*(t-\tau)] \\ &\quad + E[\varepsilon(t)x^*(t-\tau)])dt \\ &= \int_0^{T_{int}} R_{xx}(\tau - T_0)dt + \\ &\quad \int_0^{T_{int}} E[\varepsilon(t)x^*(t-\tau)]dt. \end{aligned} \qquad (12)$$

If the emitted signal $x(t)$ and the noise $\varepsilon(t)$ are independent processes then the second term in (12) is equal to zero and we get:

$$E[R(\tau)] = T_{int}R_{xx}(\tau - T_0). \qquad (13)$$

Since the autocorrelation function's maximum occurs at $\tau = 0$ ($R(\tau) \leq R(0)$), the delay T_0 can be estimated as the position of the maximum. Thus:

$$T_0 = \max_\tau |E[R(\tau)]| \qquad (14)$$

Special cases:

• Let $x(t)$ be a white stationary Gaussian random process with variance σ_x^2. The autocorrelation function is $R_{xx}(\tau) = \sigma_x^2\delta(\tau)$, where $\delta(\tau)$ is the Dirac delta function. This is an ideal shape since $E[R(\tau)] = T_{int}\sigma_x^2\delta(\tau)$, and its maxima are well defined, i.e., there is only one point different from zero. Note that signals of this form are not bandlimited and they can not be used in practical applications.

• Let $x(t)$ be a bandlimited stationary Gaussian random process with power spectral density (PSD) $S_{xx}(f) = S_0$ for $f_0 - B/2 \leq f < f_0 + B/2$ and $S_{xx}(f) = 0$ otherwise. The autocorrelation function conforms to

$$R_{xx}(\tau) = S_0 e^{j2\pi f_0 \tau} \frac{\sin(\pi B\tau)}{\pi\tau} \qquad (15)$$

with a well defined maximum at $\tau = 0$, and the first sidelobe that is $3\frac{\pi}{2}$ times lower than the main lobe.

III. Binary mask implementation

This section offers two methods of binary filtering mask implementation and, through numerical examples, assess their performances, both in the STFT and LPFT case. In all examples presented in this section, the length of the received sequence is $L = 2048$, $N = 256$ and $SNR = 0$ dB. The interference is assumed to be a sinusoidal FM signal characterized by $SIR = -20$ dB. In the LPFT calculation, the perfect knowledge of the LPFT parameters is assumed. Furthermore, only the first and second order LPFT will be herein considered.

In order to assess performances of the proposed filtering methods, i.e., to estimate a remaining interference power compared to a remaining radar signal power after a binary mask implementation, the following ratios are introduced:

$$SIR_S = 10\log_{10}\frac{\sum_{n=1}^{L}\sum_{k=1}^{N}\left|STFT_x(n,k)\,B_S(n,k)\right|^2}{\sum_{n=1}^{L}\sum_{k=1}^{N}\left|STFT_I(n,k)\,B_S(n,k)\right|^2}$$

$$SIR_{L1} = 10\log_{10}\frac{\sum_{n=1}^{L}\sum_{k=1}^{N}\left|LPFT_x^1(n,k)\,B_{L1}(n,k)\right|^2}{\sum_{n=1}^{L}\sum_{k=1}^{N}\left|LPFT_I^1(n,k)\,B_{L1}(n,k)\right|^2}$$

$$SIR_{L2} =$$

$$10\log_{10}\frac{\sum_{n=1}^{L}\sum_{k=1}^{N}\left|LPFT_x^2(n,k)\,B_{L2}(n,k)\right|^2}{\sum_{n=1}^{L}\sum_{k=1}^{N}\left|LPFT_I^2(n,k)\,B_{L2}(n,k)\right|^2} \tag{16}$$

where $B_S(n,k)$, $B_{L1}(n,k)$ and $B_{L2}(n,k)$ respectively represent binary masks obtained in the STFT, the first and second order LPFT based filtering procedures.

A. Type I binary mask

The first adopted binary mask is trivial, i.e., it is assumed to excise all frequency bins of the transform, whether corrupted by an interference or not, that exceed some threshold value. The following threshold value will be assumed:

$$\begin{aligned} T_1 &= E\left[\left|STFT_{x+\xi}(n,k)\right|^2\right] \\ &\quad +2\sqrt{Var\left[\left|STFT_{x+\xi}(n,k)\right|^2\right]} \end{aligned} \tag{17}$$

where $E[\cdot]$ and $Var[\cdot]$ respectively represent the expectation and variance operator. Clearly, $STFT_{x+\xi}(n,k)$ represents the STFT of the sum $x(n)+\xi(n)$.

The advantage of this type of binary mask is simple hardware realization. However, its drawback is the removal of a certain number of frequency bins that are not corrupted by interference. Moreover, the strongest frequency components of the radar signal are eliminated in this manner.

The first and third rows of Table I give values of the SIR ratios (see 16), averaged over 100 realizations. Binary masks for one realization of the STFT, the first and the second order LPFT based suppression of the SFM interference, denoted as $\mathbf{B_S^I}$, $\mathbf{B_{L1}^I}$ and $\mathbf{B_{L2}^I}$, are depicted in Figures 1(a), (b) and (c), respectively. Corresponding binary masks for the LFM interference case are depicted in Figures 2(a) and 2(b) with superscript I denoting the first type of binary mask. In addition, the percentage of the excised frequency bins for all the implemented transforms, averaged over 100 runs, is shown in the first and third rows of Table II. Needless to say, the second order LPFT has not been calculated into the LFM case since the first order LPFT completely focuses LFM interference in a narrow band.

B. Type II binary mask

The second adopted binary mask is more sophisticated than the first one as it removes only corrupted frequency bins around the spectral peak at the current time instant. It is obtained by means of the following steps.

Step 1. Set the binary mask $B(n,k)$ to all ones and set $n=1$.

Step 2. If $n > L$ exit; otherwise detect the maximum of $|STFT_r(n,k)|$ (or $\left|LPFT_r^M(n,k)\right|$) at the current time instant n. Let the frequency index of the maximum be k_1 and set $k_2=k_1$.

Step 3. As long as

$$\begin{aligned} &|STFT_r(n,k_2)| > |STFT_r(n,k_2-1)| \\ &\text{or } |STFT_r(n,k_2)|^2 > T_2 \end{aligned}$$

set $B(n,k_2)=0$ and iterate $k_2=k_2-1$ until step 3 is done.

Step 4. Set $k_2=k_1+1$. As long as

$$\begin{aligned} &|STFT_r(n,k_2)| > |STFT_r(n,k_2+1)| \\ &\text{or } |STFT_r(n,k_2)|^2 > T_2 \end{aligned}$$

set $B(n,k_2)=0$ and iterate $k_2=k_2+1$ until step 4 is done.

Step 5. Set $n=n+1$ and go to step 2.

Here, T_2 represents the threshold value defined as

$$\begin{aligned} T_2 &= E\left[\left|STFT_{x+\xi}(n,k)\right|^2\right] \\ &\quad +\sqrt{Var\left[\left|STFT_{x+\xi}(n,k)\right|^2\right]}. \end{aligned} \tag{18}$$

The advantage of the binary mask defined in this way is the sophisticated interference removal. We begin with a position of an interference spectral peak, at the needed time instant n, and set $B(n,k)=0$ for all frequency bins k of the transform that are corrupted by the interference. This procedure is performed as long as the absolute value of the current frequency bin is greater than the adjacent one or its squared absolute value is greater than the adopted threshold value defined by (18). Furthermore, frequency bins of the transform that are not corrupted by an interference remain

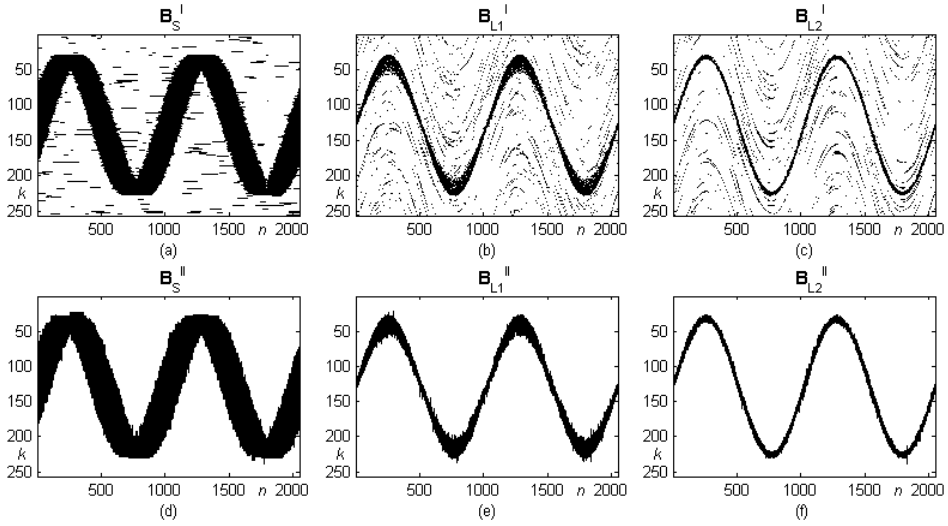

Fig. 1. Sinusoidal FM interference case. *First row*: Type I binary masks for (a) STFT, (b) LPFT^1 and (c) LPFT^2 based interference excision. *Second row*: Type II binary masks for (d) STFT, (e) LPFT^1 and (f) LPFT^2 based interference excision. Zero values are shown in black. n - time index, k - frequency index.

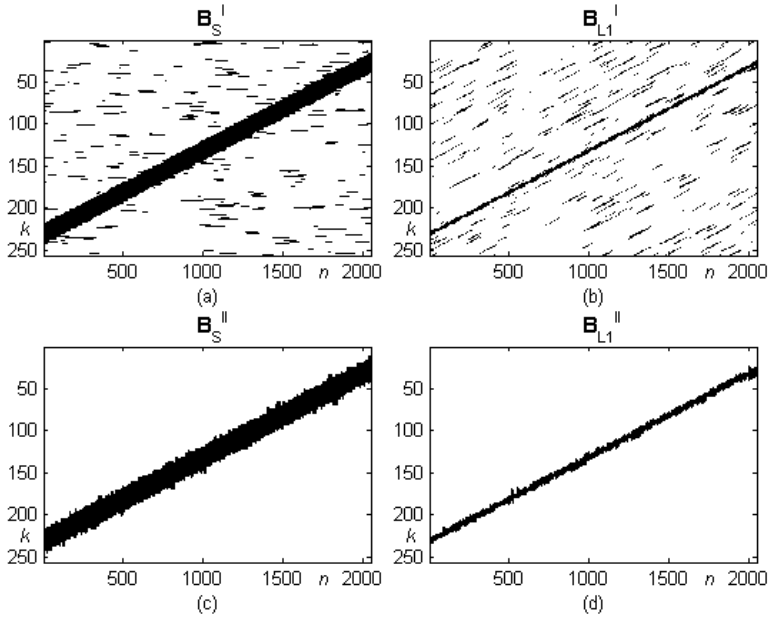

Fig. 2. LFM interference case. *First row*: Type I binary masks for (a) STFT and (b) LPFT^1 based interference excision. *Second row*: Type II binary masks for (c) STFT and (d) LPFT^1 based interference excision. Zero values are shown in black. n - time index, k - frequency index.

TABLE I
SIR IN dB FOR TYPE I AND TYPE II BINARY MASKS

Interf.	Bin. mask	STFT	LPFT[1]	LPFT[2]
Sin FM	Type I	7.49	11.66	13.76
Sin FM	Type II	16.08	20.41	25.3
Lin FM	Type I	12.62	16.58	–
Lin FM	Type II	24.1	30.88	–

TABLE II
EXCISED BINS PERCENTAGE FOR TYPE I AND TYPE II BINARY MASKS

Interfer.	Bin. mask	STFT	LPFT[1]	LPFT[2]
Sin FM	Type I	33.49%	12.03%	8.4%
Sin FM	Type II	33.32%	10.18%	6.03%
Lin FM	Type I	14.1%	6.81%	–
Lin FM	Type II	12.12%	4.11%	–

intact. The drawback of this binary mask is rather complicated hardware realization.

The second and fourth rows of Table I present obtained values of ratios (16), averaged over 100 realizations. Binary masks for one realization of the STFT, the first and second order LPFT based filtering in the sinusoidal FM interference case, denoted as $\mathbf{B_S^{II}}$, $\mathbf{B_{L1}^{II}}$ and $\mathbf{B_{L2}^{II}}$, are depicted in Figures 1(d), 1(e) and 1(f), respectively. Corresponding binary masks for the LFM interference case are depicted in Figures 2(c) and 2(d). Superscript II denotes the second type of binary mask. Again, the percentage of the excised frequency bins for all the three implemented transforms, averaged over 100 runs, is presented in the second and fourth rows of Table II.

C. Discussion

Despite the fact that the removed area is approximately the same (see Table II), the second type of binary mask is characterized by a significant improvement in SIR performance compared to the first type, as shown by results given in Table I. The reason for such a behavior is the fact that the first type of binary mask eliminates the strongest frequency components of the radar signal along with the interference components.

The STFT based filtering is outperformed by the first order LPFT based filtering, however, the second order LPFT produces the best results, since the corresponding excised area is the smallest compared to the other two. Furthermore, as can be seen from Figs. 1(f) and 2(d), the number of excised frequency bins is approximately the same for each time instant, meaning that increasing the LPFT order would not provide a significant SIR improvement.

Monocomponent interference has been assumed in this analysis. If an interference is a multicomponent signal, type I binary mask and STFT can be applied without any modifications, while the procedure for the type II binary mask implementation or LPFT needs to be modified in order to remove all interference components [16].

IV. SIMULATIONS

Consider a noise radar operating at carrier frequency $f_0 = 10\,\text{GHz}$ with bandwidth $B = 204.8\,\text{MHz}$ and pulse duration of $T_r = 10\,\mu\text{s}$ (or 2048 samples). The received signal is sampled at the Nyquist rate $T_s = 1/B$. The radar waveform is a complex Gaussian random signal with i.i.d. (independent and identically distributed) real and imaginary parts. The transmitted signal is reflected from the single point scatterer target located at distance $r_0 = 1\,\text{km}$. Let us also assume that the received signal is corrupted by a complex AWGN $\xi(t)$ and in-

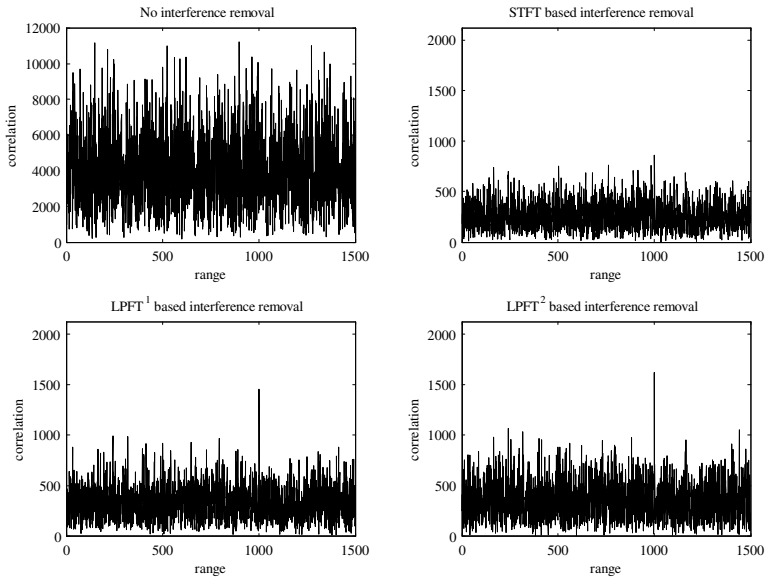

Fig. 3. Output of the correlation receiver for the single target located at 1000 m range with $SNR = -20$ dB and $SIR = -40$ dB when no filtering is performed (upper left), STFT based filtering is performed (upper right) first order LPFT filtering (lower left) and second order LPFT (lower right). Type II binary mask is used.

terference signal $I(t)$. The received signal is of the form

$$r(t) = x(t) + I(t) + \xi(t) \tag{19}$$

where $x(t) = A_x x_t(t - t_d)$ represents a signal reflected from the target, characterized by an attenuation A_x and time delay $t_d = \frac{2r_0}{c}$. Note that $r(n)$, defined by (1), represents the discrete version of (19).

The interference is assumed to be a frequency modulated signal of the form

$$I(t) = A_I e^{j\varphi_I(t)}.$$

Two types of interference are analyzed:

1) Sinusoidal FM interference, i.e., the interference with the instantaneous frequency (IF)

$$f_I^S(t) = \frac{d\varphi_I(t)}{dt} = -\frac{3}{8}B\sin(8\pi\frac{t}{T_r}). \tag{20}$$

2) Linear FM interference, i.e., the interference with the IF

$$f_I^L(t) = \frac{d\varphi_I(t)}{dt} = -2B\frac{t}{T_r}, \quad \text{for } -\frac{T_r}{4} < t < \frac{T_r}{4}. \tag{21}$$

The LFM interference is periodic with period $\frac{T_r}{2}$ and (21) is valid only within the fundamental period. Such an LFM interference may be viewed as an interfering LFM radar signal covering the same time and frequency ranges as the operating noise radar.

The interference suppression is performed by using the proposed TF based filtering of the received signal.

The following four cases are considered:

1. No interference suppression is performed.
2. Interference suppression is performed by using the STFT.
3. Interference suppression is performed by using the LPFT of the first order.
4. Interference suppression is performed by using the LPFT of the second order.

For the interference suppression, both type I and type II binary mask are used, as described in Section III. Figure 3 presents radar outputs in all the considered cases. Note that the target is not detected when no interference suppression is performed, and the LPFT based filtering outperforms the STFT based approach.

The simulations were performed over 1000 realizations of the received signal. The proba-

TABLE III
PROBABILITY OF FALSE TARGET DETECTION FOR $SNR = -20$DB AND SINUSOIDAL FM INTERFERENCE. TYPE I BINARY MASK IS USED.

SIR	No filtering	STFT	LPFT[1]	LPFT[2]
−20dB	27.7%	46.9%	15.3%	11.0%
−25dB	75.7%	57.1%	18.2%	11.4%
−30dB	96.7%	58.0%	20.0%	12.7%
−35dB	99.4%	63.1%	25.4%	16.0%
−40dB	99.5%	68.0%	30.6%	18.5%

TABLE IV
PROBABILITY OF FALSE TARGET DETECTION FOR $SNR = -20$DB AND LFM INTERFERENCE. TYPE I BINARY MASK IS USED.

SIR	No filtering	STFT	LPFT[1]
−20dB	29.4%	17.3%	8.1%
−25dB	76.6%	17.8%	7.9%
−30dB	97.4%	16.9%	7.8%
−35dB	99.6%	19.3%	8.7%
−40dB	99.9%	21.2%	8.5%

TABLE V
PROBABILITY OF FALSE TARGET DETECTION FOR $SNR = -20$DB AND SINUSOIDAL FM INTERFERENCE. TYPE II BINARY MASK IS USED.

SIR	No filtering	STFT	LPFT[1]	LPFT[2]
−20dB	28.5%	17.0%	2.1%	2.0%
−25dB	75.4%	18.0%	3.7%	2.7%
−30dB	96.3%	26.4%	5.2%	2.7%
−35dB	99.4%	36.6%	7.8%	2.9%
−40dB	99.4%	43.5%	10.4%	5.1%

TABLE VI
PROBABILITY OF FALSE TARGET DETECTION FOR $SNR = -20$DB AND LFM INTERFERENCE. TYPE II BINARY MASK IS USED.

SIR	No filtering	STFT	LPFT[1]
−20dB	29.5%	2.9%	1.5%
−25dB	76.2%	6.4%	1.8%
−30dB	96.4%	8.1%	1.9%
−35dB	99.3%	19.7%	1.9%
−40dB	99.7%	45.3%	2.7%

bility of false target detection versus SIR for $SNR = -20$dB is calculated and results are presented in Tables III and IV for type I binary mask, and in Tables V and VI for type II binary mask. False target detection occurs when the detected maxima position of the radar output does not coincide with the true target position.

As discussed in III-C, the type II binary mask outperforms the type I binary mask, and the LPFT provides better results than the STFT.

V. Conclusion

The problem of nonstationary interference suppression in noise radar systems is addressed. Towards this aim, time-varying filters based on linear TF transforms, namely STFT and LPFT, are developed. The filtering is performed in the TF domain by using a binary excision mask, which removes the nonstationary interference. Two approaches to the binary mask implementation are proposed. Numerical simulations show that the TF based time-varying filtering significantly improves the probability of target detection in severe interference environments. The best results are obtained by using the second order LPFT.

References

[1] Xu, X., and Narayanan, R.M.: 'Impact of Different Correlation Receiving Techniques on the Imaging Performance of UWB Random Noise', Geoscience & Remote Sensing Symposium, IGARSS'03, Vol. 7, July 2003, pp. 4525-4527.

[2] Lukin, K.A.: 'Developments of Noise Radar Technology in LNDES IRE NASU', First International Workshop on the Noise Radar Technology, NTRW 2002 Proceedings, Yalta, Ukraine, Sept. 2002, pp. 90-96.

[3] Axelsson, S.R.J.: 'On the Theory of Noise Doppler Radar', Geoscience and Remote Sensing Symposium Proceedings 2000, Honolulu, USA, pp. 856-860.

[4] Axelsson, S.R.J.: 'Noise Radar For Range/Doppler Processing and Digital Beamforming Using Low-Bit ADC', IEEE Trans. on Geoscience and Remote Sensing, Vol. 41, No. 12, Dec. 2003, pp. 2703-2720.

[5] Lukin, K.A.: 'The Principles of Noise Radar Technology', First International Workshop on the Noise Radar Technology, NTRW 2002 Proceedings, Yalta, Ukraine, Sept. 2002, pp. 13-22.

[6] Bell, D.C., and Narayanan, R.M.: 'Theoretical Aspects of Radar Imaging Using Stochastic Waveforms', IEEE Trans. on Signal Processing, Vol. 49, No. 2, pp. 394-400.

[7] Stephan, R., and Loele, H.: 'Theoretical and Practical Characterization of a Broadband Random Noise Radar', Dig. 2000 IEEE MTT-S International Microwave Symp., Boston, MA., pp. 1555-1558.

[8] Narayanan, R.M., Xu,Y., Hoffmeyer, P.D., and Curtis, J.O.: 'Design, performance, and applications of a coherent ultrawideband random noise radar', Optical Engineering, Vol. 37, No. 6, June 1998, pp. 1855-1869.

[9] Lukin, K.A.: 'Millimeter wave noise radar technology', Proc. 3rd Int. Kharkov Symp., Physics and Engineering of Millimeter and SubmillimeterWaves, Kharkov, Ukraine, pp. 94-97.

[10] Garmatyuk, D.S., and Narayanan, R.M.: 'Ultrawideband continuous-wave random noise arcSAR', IEEE Trans. on Geoscience and Remote Sensing, Vol. 40, No. 12, pp. 2543-2552.

[11] Xu, Y., Narayanan, R.M., Xu, X., and Curtis, J.O.: 'Polarimetric processing of coherent random noise radar data for buried object detection', IEEE Trans. on Geoscience and Remote Sensing, Vol. 39, No. 3, pp. 467-478.

[12] Thayaparan, T., Stanković, L., and Daković, M.: 'Mutual Interference and Low Probability of Interception', International Radar Symposium, IRS 2007, Cologne, Germany, September 2007, pp. 576-579.

[13] Thayaparan,T. and Wernik, C.: 'Noise Radar Technology Basics', DRDC Ottawa, TM 2006-266.

[14] Stanković, Lj.: 'On the time-frequency analysis based filtering', Annales des Telecommunications, Vol.55, No.5-6, May 2000, pp.216-225.

[15] Hlawatsch, F., and Boudreaux-Bartels, F.: 'Linear and quadratic time-frequency signal representations', IEEE Signal Processing Magazine, Vol.9, Apr. 1992, pp. 21–67.

[16] Stanković, Lj., and Djukanović, S.: 'Order adaptive local polynomial FT based interference rejection in spread spectrum communication systems', IEEE Transactions on Instrumentation and Measurement, Vol.54, Dec. 2005, pp. 2156-2162.

[17] Katkovnik,V.: 'A new form of the Fourier transform for time-varying frequency estimation', Signal Processing, Vol.47, no.2, pp. 187-200.